RSC Advances

ROYAL SOCIETY OF CHEMISTRY

www.rsc.org/advances

Preparation and Defluorination Mechanism of a Novel Copolymerized Hydroxyapatite-aluminium Chloride Material

Lianyuan Gong and Li Feng*

Key Laboratory of Coal Processing and Efficient Utilization of Ministry of Education, School of Chemical Engineering and Technology, China University of Mining and Technology, Xuzhou 221116, Jiangsu, China;

National Engineering Research Center of Coal Preparation and Purification, Xuzhou 221116, Jiangsu, China

*Corresponding author: Tel: +86 13852488050; E-mail: cumthgfl@163.com

Abstract: As an attempt to avoid the low defluoridation capacity of conventional adsorbents, this paper offers a novel copolymerized hydroxyapatite-aluminum (HAP-PAC) adsorbent and evaluates its performance in fluoride removal of drinking water, and a possible fluoride removal mechanism is proposed based on the characterized results obtained by FTIR, XRD, BET, SEM and EDS. The results indicate that copolymerization material prepared by crystallization of aluminum chloride is featured by the chemical combination between hydroxyapatite (HAP) and poly aluminium chloride (PAC), and certain amount of Ca^{2+} and OH^- in HAP crystal lattice are partially doping replaced by Al^{3+} and Cl^- in PAC, the structure of copolymerization material shows a uniform trend. Plus, mainly by chemical adsorption, the highest defluoridation capacity (DC) of the copolymerization material can reach up to 18.12 mg/g, an increase of 14.02 mg/g as compared with conventional hydroxyapatites. When aluminum chloride is replaced by bauxite in the study, the highest DC is 13.72 mg/g due to the co-occurrence of chemical and physical combinations and relatively lower homogeneous structure caused by the co-existence of HAP and PAC while electrostatic attraction and chemical adsorption are both involved. As for the material prepared by physical mixing method, in which the combination between HAP and PAC is mainly dominated by physical effects, its maximum DC is 13.08 mg/g, with physical adsorption as its main form of defluoridation.

Keywords: hydroxyapatite, poly-aluminum chloride, defluoridation capacity, mechanism of defluoridation

1 Introduction

Fluorine is an essential micronutrient for calcium and phosphorus metabolism in human body [1-2]. Its intake mainly comes from drinking water. An appropriate amount of fluorine can increase the hardness of bones and teeth, promote the metabolism of enzyme system and help to transfer nerve excitement [3]. However, when the level of fluoride is more than 1.5 mg/L, it can lead to various diseases, such as skeletal and dental fluorosis [4-5]. Therefore, it is significant to explore ways to reduce excessive fluoride in drinking water.

Adsorption is widely applied nowadays to remove excessive fluorine in drinking water due to its simple operation on instruments and low running cost [6-7], and the kernel for this method is the choice of an appropriate adsorbent. Popular adsorbents include activated alumina [8-9], bone charcoal [10], biological macromolecule fluoride agent [11], kaolin [12], hydroxyapatite [13-14], etc. Of all the adsorbents, activated alumina, widely employed several years ago, is seldom used now because of its low defluoridation capacity (DC), which consequently leads to a lot of regenerations and secondary pollution by adding chemical reagents, and the need to adjust the values of pH of the water system, which increases the complexity of its normal usage. In order to improve the adsorption efficacy of activated alumina, researchers have tried to modify the surface of alumina. For instance, La^{3+}-modified activated alumina (La-AA) were studied by Jiemin Cheng et al. [15]. The comparison of adsorption characteristics of the La-AA and the original alumina in the removal of fluoride concluded that the maximum DC of AA and La-AA were 2.74 and 6.70 mg/g at pH=7.0 respectively. A novel adsorbent of sulfate-doped Fe_3O_4/Al_2O_3 nanoparticles with magnetic separability was prepared, characterized and applied by Liyuan Chai et al. [16]. Test results showed that this adsorbent for fluoride by two-site Langmuir model was 70.4 mg/g at pH=7.0 with initial fluoride concentration of 160 mg/L. Bansiwal et al. [17] examined copper oxide coated alumina (COCA) by impregnating alumina with copper sulphate solution followed by calcination at 450 °C in presence of air. The

analysis indicated that the DC of COCA obtained through the Langmuir model was 7.22 mg/g, which was advanced by 5.0 mg/g as compared with unmodified AA. One disadvantage of these adsorbents is that certain amount of aluminum dissolves in the water in the defluorination process, which poses potential threat to human health in long-term drinking.

Hydroxyapatite (HAP), as new type of fluoride removal material, is superior to activated alumina in terms of its high fluoride removal capacity and availability. However, its unfixed property can induce turbidity, water filtration difficulty and the reactivation process of HAP is also extremely complex. To solve these problems, Weihua Xu et al. [18] studied a novel kind of high hardness granular filter material made by hydroxyapatite with modification of attapulgite. But this material has lower DC because of its smaller contact area with water system. Then Li Feng et al.[19] reported a method of heat regeneration of hydroxyapatite/attapulgite composite beads for defluoridation of drinking water and the its total DC can reach up to the level of powder material of HAP. Another adsorbent of alginate bioencapsulating nano-hydroxyapatite (n-HApAlg) synthesized by Pandi, K et al.[20] has higher DC (3.87 mg/g) than the original n-Hap (1.296 mg F^-/g) and calcium alginate (CaAlg) composite (0.68 mg F^-/g). Yulun Nie et al. [21] stated that aluminum modified calcium hydroxyapatite (Al-HAP) nanoparticles produced by co-precipitation method possessed higher DC of 32.57 mg/g with initial fluoride concentration of 10 mg/L. Adsorption capacity of nano-material can be increased because of its huge specific surface area. Nevertheless, its difficulty in interception can not eliminate the possibility of entering human body. Additionally, its fluoride removal capacity is greatly influenced by the concentration of fluorine-containing water: the higher the concentration is, the larger the capacity will be [19].

Poly aluminium chloride (PAC), as an inorganic polymer flocculation, is commonly applied in wastewater treatment owing to its such advantages as strong coagulability, big floc, less dosage, high water purification efficiency, etc.

This study proposes a new sorbent of HAP-PAC copolymerization material based on the analysis of fluoride removal of HAP/active aluminum and flocculation effects of PAC. Because of its high DC, it is capable of removing fluoride intensively and producing drinkable water without any health concern.

2 Materials and methods

2.1 Chemicals and materials

NaF and all other reagents used in this study were of analytical grade and they were purchased from Shanghai Chemical Corporation, China; poly aluminium chloride (PAC) from Shandong Zhongke Tianze Water Purification Materials Co., Ltd and its effective substance content (Al_2O_3) was 28%; The main ingredients of bauxite were Al_2O_3 (53.87%), SiO_2 (18.13%), and Fe_2O_3 (9.53%).

2.2 Characterization

Examination with a scanning electron microscope (SEM) (FEI Quanta250 model) fitted with an energy dispersive X-ray analyzer (EDS) allowed a qualitative detection and localization of elements within the samples. X-ray powder diffraction (XRD) patterns were obtained using a Bruker D8 AdvanceX-ray diffractometer using Cu Kα radiation, a nickel filter, and a LynxEye detector. FTIR spectra of the copolymerization materials were recorded on Nicolet 380 FTIR Spectrometer to confirm the presence of functional groups.

2.3 Preparation of Filtering Material

(1) Preparation of HAP- PAC Copolymerization Material

I. Method No.1 Crystallization of Aluminum Chloride ($AlCl_3 \cdot 6H_2O$) for the Raw Material

First, certain amount of $AlCl_3 \cdot 6H_2O$ was weighed and put into a muffle furnace with temperature set at 290 °C. After being heated for 30 min, it was stirred with the addition of certain amount of distilled water, during which some sticky resin material, namely semi-finished PAC, was produced. After this process, some sample of this material was taken and its content of Al_2O_3 was titrated according to National Standard Method (HG/T 2677-2009). Then, after the instilment of phosphoric acid, an appropriate amount of the semi-finished PAC was

added to the synthesis reaction of HAP [22], a process that accompanied the preparation of the semi-finished PAC. After 60 min maturation at the temperature of 90 °C, the sample was taken out and cooled down to room temperature naturally. Then it was filtered, washed, dried for 12 hours at the temperature 105 °C, and then grinded. Finally the material prepared under these optimized conditions was, for the convenience of study, labeled as H1.

II. Method No.2 Bauxite as the Raw Material

First, Bauxite was smashed and sieved by 100 mesh sieve. Afterwards, certain amount of bauxite was weighed and put into a muffle furnace. After being heated for 60 min with the temperature set at 650 °C, the calcined bauxite and certain amount of 20% HCl solution was put into three-necked flask and mixed, the ratio of the bauxite mass and the HCl volume was 1:1.5. The next step was acid solution, in which allihn condenser reflux was adopted to conduct backflow, with the temperature of pickling from 85 °C ~ 95 °C and a duration for 2 hours. After this stage, appropriate amount of $NaAlO_2$ was slowly added to conduct polymerization that lasted for 4 hours at the temperature 90±2 °C (the mass ratio of the bauxite and $NaAlO_2$ was 5:1). After cooling down to room temperature naturally, the processed material was filtered to obtain the liquid PAC. Then some sample was taken and its Al_2O_3 content was titrated based on National Standard Method (HG/T 2677-2009). An appropriate amount of the newly-produced liquid PAC was added to the synthesized HAP when the dripping of phosphoric acid finished during the synthesis of HAP [22], a process concurrent with the preparation of the liquid PAC. After the maturation of this mixture for 60 min at 90 °C, some of the mixture was sampled and cooled down to room temperature naturally. Then it was filtered, washed, dried for 12 h at the temperature 105 °C, and then grinded. Finally material prepared under these optimal conditions was labeled as H2.

(2) Method No.3 HAP and PAC Physical Mixing

The prepared HAP [22] and PAC (commercially available) were mixed according to certain mass ratio and the sample produced under these ideal conditions was labeled as H3.

2.4 Batch Adsorption Experiments

A 5 mg/L fluoride solution was prepared by dissolving 0.1105 g of NaF in tap water for a volume of 10 L to be used as the fluoride-containing water sample.

The prepared water sample was transferred into coagulation blender container till the volume reached 0.6 L. Then 0.09 g filtering materials was added into the container, which was followed by stirring at the speed of 200 r/min for 30 min. After maturating for 30 min, 25 mL of supernatant was pipetted to volumetric flask labeled with 50 mL, and 10 mL of TISAB solution added. During the whole process their volume was maintained. At last, electromotive force E of the solution was tested by fluoride ion-selective-electrode, pF-1 (made in China). A standard curve could be drawn by setting electromotive force E of standard solution as Y-axis whereas logarithm of solution concentration as X-axis, that was y=-57.071x+235.23 with correlation index R^2=0.9999. Then the concentration (mg/L) of fluoride ion in the solution could be calculated based on this curve.

3 Results and Discussion

3.1 The Effect of Al/Ca Molar Ratio on Fluoride Removal

The Al/Ca molar ratio is applicable to the characterization of the molar ratio between Al element measured by Al_2O_3 in PAC and Ca element in HAP. Filtering materials are prepared by physical mixing set molar ratio of Al/Ca as 0, 0.022, 0.044, 0.088, 0.132, 0.176, 0.22, 0.264, and 0.308 respectively. The effects of different Al/Ca molar ratio on the adsorption capacity are evaluated by the defluoridation capacity (DC) and the results are shown in Fig. 1.

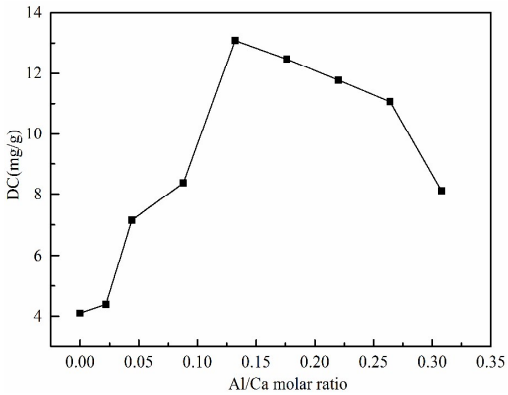

Fig. 1 The effects of different Al/Ca molar ratio on defluoridation capacity on physical mixing

As the Fig. 1 shows, the DC of pure HAP is 4.10 mg/g, and its capacity shows no distinct variation as a small quantity of PAC is added to make the ratio turn into 0.022. It then rises quickly from 0.022 to 0.132 and possesses the maximum DC of 13.08 mg/g when the Al/Ca molar ratio is 0.132. However, the DC will decrease with the further increase of Al/Ca molar ratio. The possible explanation for this phenomenon lies in the fact that certain kind of synergistic effect between HAP and PAC may be induced with the increase of Al/Ca molar ratio, thus improving the capacity of defluoridation. Moreover, the flocculation precipitation caused by the flocs from PAC and turbidity from fluor-hydroxyapatite accelerates the adsorption reaction between adsorbent and fluoride in water, which in turn mitigates the potential dangers of turbidity value decrease in water and aluminum dissolved in PAC. It can be seen that the filtering material with the best proportion exhibits the highest efficiency for the removal of fluoride. As ratio increases beyond the optimal one, further addition of the PAC means more impurities to the filtering material, which lowers its adsorption ability thus weakening its DC.

Fig. 2 shows impact on DC as filtering materials prepared by chemical synthesis under different Al/Ca molar ratio. The preparation methods are divided into crystalline aluminum chloride ($AlCl_3 \cdot 6H_2O$) method and the bauxite method due to the difference in the choice of the raw materials.

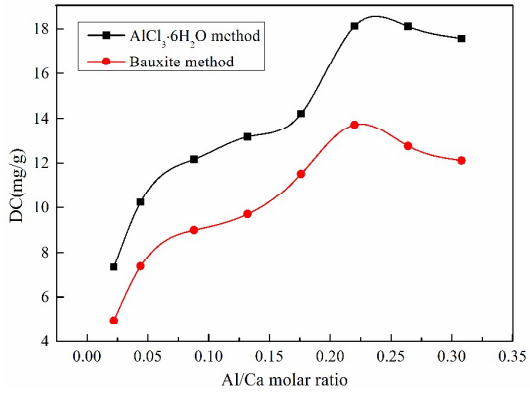

Fig. 2 The influence of different Al/Ca molar ratio on defluoridation capacity on chemical synthesis

It can be observed from Fig. 2 that the overall trend of the two curves displays some similarity. That is, the fluoride removal capacity will increase firstly and then decrease with the increase of Al/Ca molar ratio, and the DC of bauxite method is relatively lower. An account for this is that the two filtering materials form a stable structure when copolymerization occurs between special amounts of HAP and PAC in the preparation process, which leads to their relatively higher DC. However, this intensification in DC can be weakened as excessive physical mixture arises between them. As compared with $AlCl_3 \cdot 6H_2O$ method, the effective content of the prepared product is relatively lower in view of the high content of impurities in raw bauxite, which triggers its poor effect of copolymerization with HAP. Consequently, the adsorption capacity of the filtering material generated by bauxite method is not as effective as that created by $AlCl_3 \cdot 6H_2O$ method. Optimal Al/Ca molar ratio of filtering materials produced by $AlCl_3 \cdot 6H_2O$ method and bauxite method demonstrates identical value 0.22，and

corresponding DC are 18.12 mg/g and 13.72 mg/g respectively. Both methods increase the DC by 14.02 mg/g and 9.62 mg/g respectively over conventional hydroxyapatite.

3.2 Characterization of Adsorbents

3.2.1 FTIR Analysis

The functional group structures of H1, H2, H3 and pure HAP, PAC are characterized via FTIR and the infrared spectra is shown in Fig. 3.

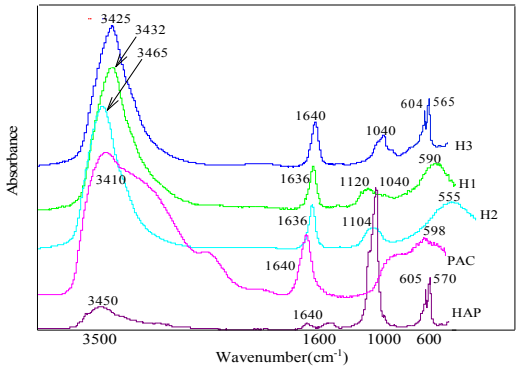

Fig. 3 FTIR spectra of filtering materials

(In Fig. 3: H1 is the copolymerization material prepared by $AlCl_3 \cdot 6H_2O$; H2 is the filtering material prepared by bauxite; H3 is the filtering material prepared by physical mixing method)

Fig. 3 indicates that HAP shows a strong P-O stretching vibration peak at 1040 cm^{-1} and a P-O bending vibration double peak at 605 cm^{-1} and 570 cm^{-1}. Additionally, HAP also presents a relatively weaker -OH stretching vibration peak at 3450 cm^{-1} and a relatively weaker -OH bending vibration peak at 1640 cm^{-1}. The characteristic peaks of PAC are listed as below. A relatively stronger broad peak at 3410 cm^{-1} and a relatively stronger sharp peak at 1640 cm^{-1} are respectively ascribed to the stretching vibration and bending vibration of -OH. The characteristic peak at 598 cm^{-1} is assigned to bending vibration of Al-Cl.

In comparison with the infrared spectra of pure HAP and PAC, both the spectra of H1 and H2 at near 3410 cm^{-1} and 1640 cm^{-1} show relative stronger -OH stretching vibration and bending vibration peaks, which are similar to those of PAC. Even so, it is worth noting that the red shift occurs at 3410 cm^{-1}, so does the blue shift at 1640 cm^{-1}, and their wavenumbers display slight difference. The results suggest clearly that the material structure is different from that of the pure HAP and PAC. While a relatively higher P-O stretching vibration peak, which is similar to HAP in this aspect, appears at near 1040 cm^{-1}, the band exhibits obvious shift to higher wavenumbers when the intensity of the absorption peak decreases significantly and the wavenumber changes slightly. This may be due to the bending vibration of the Al-OH-Al groups. In addition, the single peaks respectively at 604 $cm^{-1}$and 565 cm^{-1} may be attributed to the bending vibration of the O=P···Cl groups. Part of hydroxyl in HAP may be replaced by Cl in PAC. On the basis of aforementioned results, it can be said that the chemical action plays a dominant role in the synthesis of H1 and H2 and that the degree of the action and the results display slight differences.

The spectra of H3 at 3425 cm^{-1} and 1640 cm^{-1} have the relative stronger stretching vibration and bending vibration peaks of -OH group, which bears certain similarity to PAC at 3410 cm^{-1} and 1640 cm^{-1}. The change of the wavenumber at 3425 cm^{-1} may be the result of the overlap of peaks between PAC and HAP. There are also a relatively higher P-O stretching vibration peak, which is also shown in HAP at 1040 cm^{-1}, and, just like HAP, doublets at 604 cm^{-1} and 565 cm^{-1}. The change of wavenumbers may be attributed to the overlap of peaks at 598 cm^{-1}. On the grounds of aforementioned results, it can be concluded that physical action plays an important role in the formation procedure of H3 but does not change the respective structures of HAP and PAC.

3.2.2 XRD Analysis

The crystal structures of the pure HAP and HAP-PAC copolymerization material are characterized by the X-ray diffraction. The results are represented in Fig. 4.

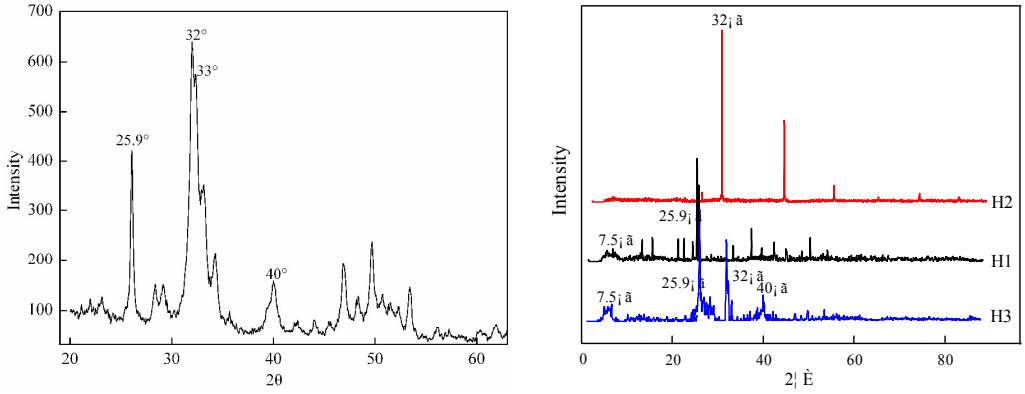

(a) (b)

Fig. 4 XRD spectra of powder HAP (a) and filtering materials (b).

The XRD patterns of Fig. 4 (a) shows that the crystalline peaks at 2θ= 25.9°, 32°, 33°, 35.5° and 40°, which confirms the formation of hydroxyapatite structure. Based on existing data, characteristic peaks of PAC are 7.5°, 8.3°, 10.2°, 10.8°, 12.7°, and 13.5° respectively [23]. In comparison with Fig. 4 (a) and Fig. 4 (b), it can be found that filtering materials H1 and H2 have different characteristic diffraction peaks with pure HAP or PAC. Evidence obtained from XRD study suggests that these synthesized filtering materials have changed their respective molecular structures of HAP and PAC. However, formation procedure of filtering material H3 does not alter the respective structures of HAP and PAC because multiple HAP and PAC characteristic peaks are found in H3. This means that the mixing between these two materials mainly belongs to a physical measure, which conforms to the information as reflected by FTIR spectra.

As can be seen in Fig. 4 (b), crystallization degree of H3 is the lowest with relatively more impurity peaks, while those of H1 and H2 are relatively higher. The peak shape is extremely sharp, the peak width higher and narrower, and the background thinner. The results imply that chemical reaction is able to enlarge the grains crystals of H1 and H2, and stimulate the decrease of crystal defect and intercrystalline disordered structure, which further demonstrates that structures of H1 and H2 are more evenly distributed than that of H3.

3.2.3 BET Analysis

BET results are presented in table 1, it can be seen that H1 owns the largest specific surface area and the optimal averaging chemical mixture, which is consistent with its highest defluoridation capacity. The specific surface area of H2 and H3 shows little difference with each other due to the fact that both of their mixture modes are nonuniform, that is the physical mixture mode, then there is no doubt that their defluoridation capacity shows no great difference. Nonetheless, FTIR and XRD analysis indicate that H2 also contains certain chemical reactions. Hence, H2 possesses relatively higher defluoridation capacity than that of H3. In conclusion, the BET results shows high degree of consistency with the results obtained from static adsorption experiment.

Table 1 The results of BET analysis

Adsorbent	$a_{s,BET}$ (m^2/g)	Average pore diameter (nm)	Total pore volume (cm^3/g)
H1	43.807	5.206	0.057
H2	22.783	4.305	0.025
H3	28.429	12.844	0.091

3.2.4 SEM with EDS Analysis

The analysis of the morphology and structure in the thin surface layers are tested by SEM with EDS. The SEM micrographs of these three filtering materials are respectively presented in Fig. 5. By comparing these three

images, it is clear that the structure of H1 is relatively uniform and there are no obvious HAP and PAC particles, which testifies that HAP and PAC in H1 can chemically form HAP-PAC specified by uniform copolymer, regular structure and higher copolymerization degrees. But there are obvious particles with varying sizes and irregular shapes in H3 thus demonstrating that what occurs in H3 is mainly a physical process when HAP and PAC are mixed, and that the respective structures of HAP and PAC undergo no changes during the preparation of them. Therefore, H3 shows a general non-uniform structure. The shape and particle size of H2 are in their intermediate state and there are multiple non-uniform particles. The size of the particles is also smaller than that of H3, which leads to the conclusion that there is certain chemical reaction during the preparation of H2, though it is not sufficient enough. Besides, this procedure is accompanied by certain physical mixture and there are multiple ingredients in H2.

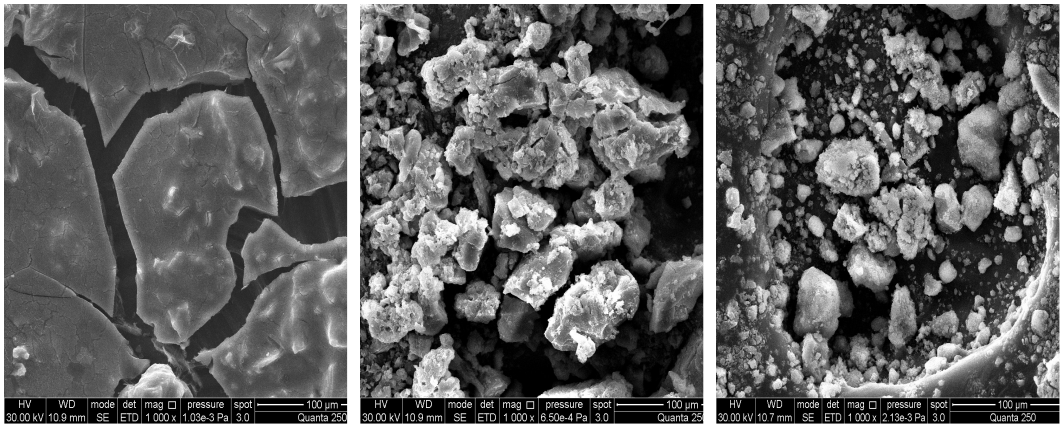

(a) (b) (c)

Fig. 5 SEM images of H1 (a), H2 (b), and H3 (c).

EDS area-scan diagram and EDS line-scan diagram of H1, H2, and H3 are displayed in Fig. 6 (a), (b), (c). EDS line-scan diagram indicates that all surfaces of H1, H2, and H3 contain elements Ca, Al, Cl, P, and O. Surface scanning energy spectrum in Fig.6 (a) and Fig.6 (b) suggest that the morphological structures of all elements but oxygen show identical trend and they are uniformly distributed on the surfaces of H1/H2. This proves that elements in H1 and H2 are specified by homogeneous distribution and stable combination. In view of the alternation of FTIR functional groups and preparation process, it can be speculated that copolymerization occurs between HAP and PAC and that the possible combination form for this procedure is that certain amount of Ca^{2+} and OH^- in HAP crystal structure is partially doped and replaced by Al^{3+} and Cl^- in PAC. Elements Ca and P in H3 display identical morphology and structure, so does Al and Cl. However, the morphology and structure between these two groups is apparently different, which indicates Ca and Al in the filtering material are unevenly distributed. On the basis of preparation process, conclusion can be drawn that HAP and PAC are physically mixed with each other during the synthetic process and that there is no occurrence of copolymerization reaction. The information reflected is consistent with the FTIR and XRD.

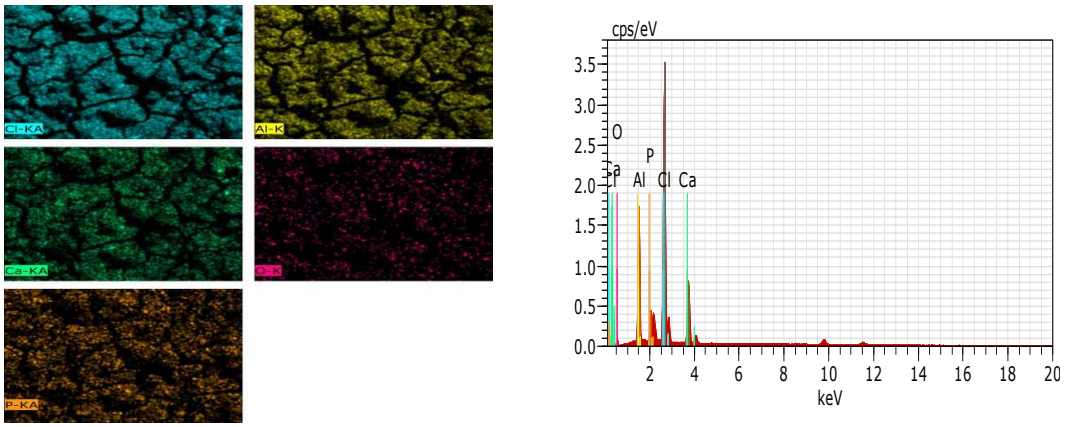

Fig. 6 (a) EDS spectrum for copolymerization material H1

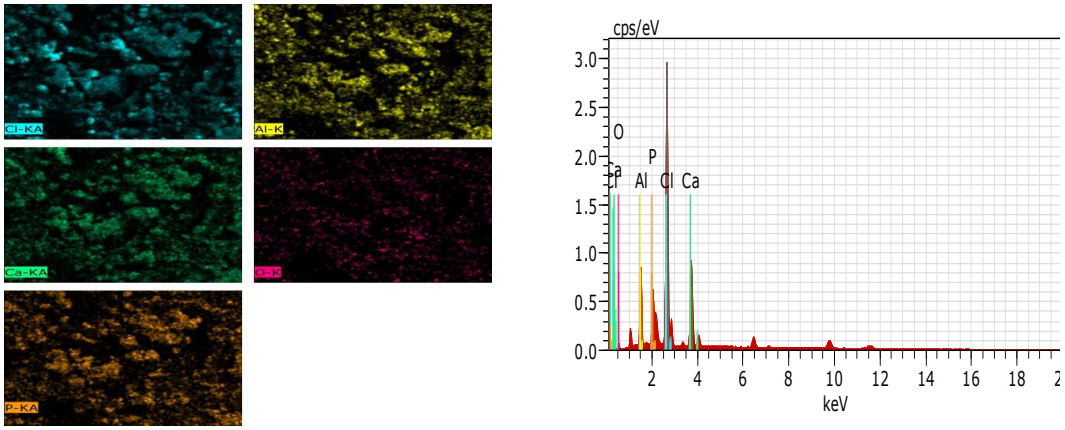

Fig. 6 (b) EDS spectrum for filtering material H2

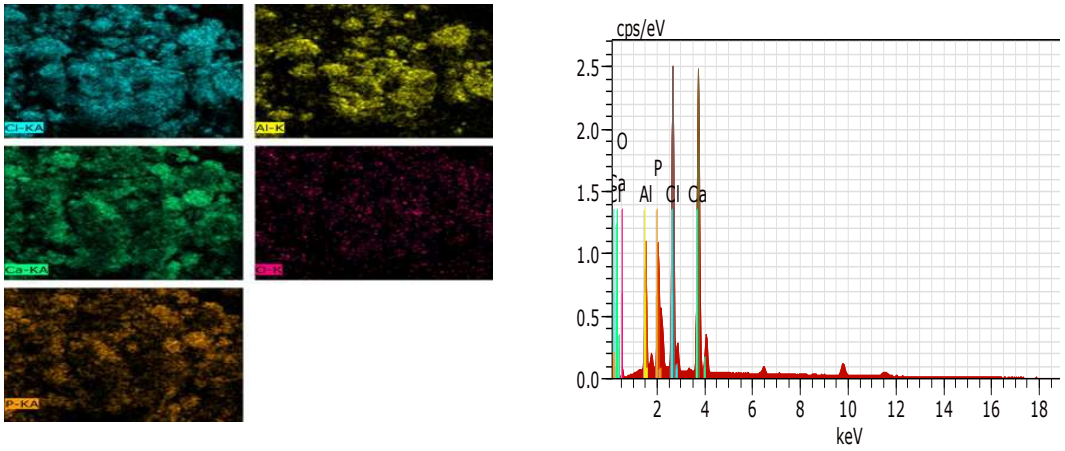

Fig. 6 (c) EDS spectrum for filtering material H3

3.3. Adsorption Kinetics and the Effects of pH

The kinetics of adsorption is an important parameter for designing adsorption system and is required for selecting optimum operating conditions for full-scale batch process. The different parameters of adsorption kinetics onto these three filter materials are illustrated in Fig. 7. In our study, the kinetic data of H1, H2 and H3 fit well with pseudo-second-order equation, the adsorption process of them generally belongs to chemical adsorption[24]. From the shape of the kinetic curve, it is evident that the fluoride adsorption onto HAP-PAC copolymerization material is a two-step process, i.e. initial rapid adsorption during the first 25 min and slow rate of adsorption until the equilibrium is reached. The pseudo-second-order equation is shown below.

$$\frac{t}{Q_t} = \frac{1}{k_2 Q_e^2} + \frac{1}{Q_e} t$$

Where Q_t is the amount of fluoride on the surface of filter materials at any time (mg/g), k_2 is the pseudo-second-order rate constant (g/mg. min), Q_e is the amount fluoride adsorbed at equilibrium (mg/g) and t is the reaction time (min).

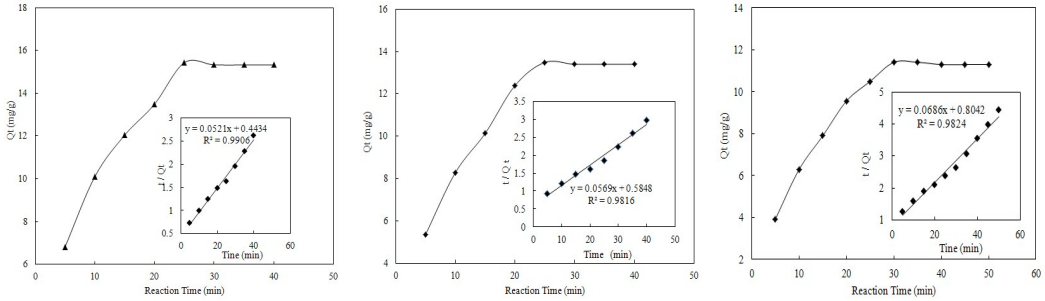

(a) (b) (c)

Fig. 7. Pseudo-second-order adsorption rate of F^- adsorption onto H1 (a), H2 (b) and H3 (c).

The pH of the medium is one of the important variables which significantly affect the extent of adsorption of fluoride. Fig. 8 shows the effect of the initial solution pH on the fluoride adsorption onto H1, H2 and H3 at given conditions. Obviously, the maximum defluoridation capacity (DC) is recorded at pH=5.69 and shows gradual decreasing trend with increase in the solution pH. The reduction of fluoride removal in alkaline pH range should be attributed to competition of hydroxyl ions with fluoride for adsorption sites because of similarity in fluoride and hydroxyl ions in charge and ionic radius.

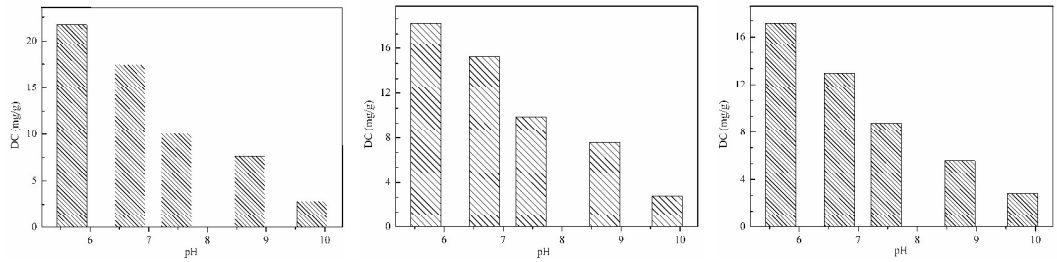

(a) (b) (c)

Fig. 8 Defluoridation capacity onto H1 (a), H2 (b) and H3 (c) at various initial pH values

3.4 Adsorption Isotherm

Analysis of equilibrium data is important for developing an equation that can be used to compare different adsorbents under different operational conditions and to design and optimize an operating procedure. The adsorption isotherms of these three filtering materials are shown in Fig. 9.

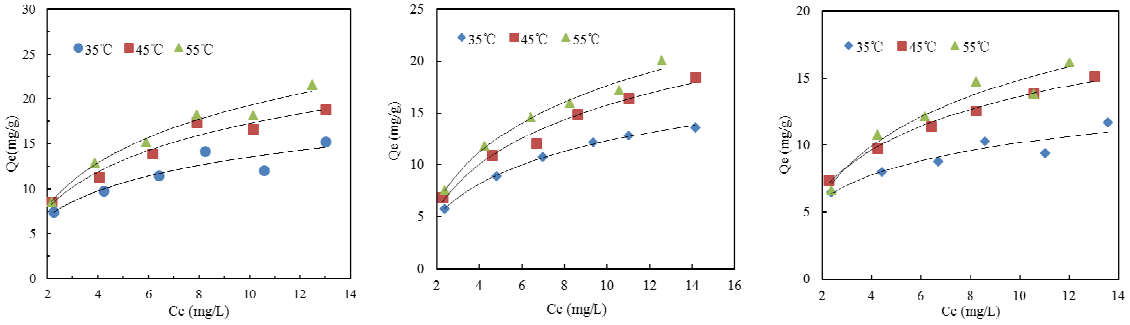

(a) (b) (c)

Fig. 9 Adsorption isotherms of H1 (a), H2 (b) and H3 (c) at different temperature

Data from the adsorption isotherms are modeled using the Langmuir and Freundlich isotherm models with the resulting isotherm constants presented in Table 2.

$$\frac{1}{Q_e} = \frac{1}{Q_m a} * \frac{1}{C_e} + \frac{1}{Q_m} \quad \text{Langmuir model}$$

$$\log Q_e = \log K_F + \frac{1}{n} \log C_e \quad \text{Freundich model}$$

Where C_e is equilibrium concentration (mg/L), Q_e is the amount adsorbed at equilibrium (mg/g), Q_m is adsorption capacity for Langmuir isotherms and 'a' is an energy term which varies as a function of surface coverage strictly due to variations in the heat of adsorption. 'n' indicates the degree of favorability of adsorption and K_F is the isotherm constant for Freundich model.

Table 2 Langmuir and Freundlich isotherm constants for F^- adsorption by filtering materials

Adsorbent	Adsorption model	Relevant parameter	308K	318K	328K
H1	Langmuir	Q_m(mg/g)	19.194	24.876	32.030
		a	0.181	0.168	0.144
		R^2	0.9997	0.9884	0.9772
	Freundlich	n	2.045	1.873	1.814
		K_F	3.973	4.575	4.974
		R^2	0.9781	0.9869	0.9772
H2	Langmuir	Q_m(mg/g)	17.544	23.866	29.412
		a	0.318	0.25	0.191
		R^2	0.9396	0.974	0.9914
	Freundlich	n	2.599	2.211	2
		K_F	5.562	6.109	6.142
		R^2	0.8972	0.9647	0.9704
H3	Langmuir	Q_m(mg/g)	12.180	20.202	24.450
		a	0.469	0.246	0.163
		R^2	0.9183	0.9526	0.9233
	Freundlich	n	3.293	2.149	1.985
		K_F	5.033	5.018	4.711
		R^2	0.9152	0.9572	0.9242

As seen in Fig. 9 and Table 2, fluoride adsorption onto H1 is well described by the Langmuir model. It indicates that homogeneous distribution of active sites on the adsorbents surface and the adsorption of fluoride takes place in a monolayer adsorption manner. Langmuir model of H2 is not as good as that of H1 on account of the participation of physical adsorption in H2. H3 is well described by the both model, it indicates that H3 is dominated by physical adsorption, and it only belongs to Langmuir model when the pores are sufficiently small. Furthermore, as the temperature increases from 35 ℃ to 55 ℃, a positive effect is observed on the adsorption of fluoride (Table 2). This phenomenon is because of the increased tendency of fluoride attached to filtering materials, which may also indicat that the adsorption of fluoride onto filtering materials is endothermic in nature. In order to study the feasibility of the process, the thermodynamic parameters are obtained from the following equations:

$$\Delta G^{\theta} = -RT\ln K^{\theta}$$

$$\ln K = \frac{\Delta S}{2.303R} - \frac{\Delta H}{2.303R}\cdot\frac{1}{T}$$

The value of K^{θ} can be obtained from the intercept of a plot of ln (Q_e /C_e) vs. C_e, which C_e is equilibrium concentration (mg/L), Q_e is the amount adsorbed at equilibrium (mg/g). The values of $\triangle H^{\theta}$ and $\triangle S^{\theta}$ can be obtained from the slope and intercept of a plot of ln$K$ vs. 1/T and the results are represented in Table 3. The adsorption of fluoride onto H1, H2 and H3 are endothermic in nature.

Table 3 Thermodynamic parameters for F^- removal on filtering materials

Adsorbent	Temperature	K	ΔG (kJ/mol)	ΔH (kJ/mol)	ΔS (J/mol.K)
H1	308K	2.017	-1.796	27.889	81.796
	318K	2.181	-2.061		
	328K	2.308	-2.281		
H2	308K	1.300	-0.672	14.246	51.490
	318K	1.451	-0.954		
	328K	1.505	-1.047		
H3	308K	1.102	-0.248	9.571	33.345
	318K	1.239	-0.548		
	328K	1.243	-0.557		

3.5 Mechanism of Fluoride Removal by the Sorbents

The defluoridation process of HAP-PAC copolymerization material is extremely complicated. In view of multiple evaluations, comparisons among infrared spectra, analyses on surface morphology of filtering materials, and related research on fluoride removal, it can be reasoned that the formula of copolymerization material is $[Al_xCa_{10-x}(PO_4)_6Cl_y(OH)_z]^{(x+2-y-z)+}$, and from the result of the influence of pH value we can know that the M-OH on the surface of filtering materials belong to active sites. It can also be concluded that the quantitative substitution of the M-OH groups by F^- plays a key role in F^- adsorption [21].The more adsorption sites are formed on HAP-PAC copolymerization material, which possesses abundant surface hydroxyl groups and the more efficient F^- removal. However, the anion exchange has happened during the modified process, when hydroxide ion is dissociated from Ca-OH, elevating the pH value. Under this circumstance, aluminum ion can combine with hydroxyl ion, forming tetrahydroxoaluminate ion, and the ion-exchanging reaction can arise happen between HAP and tetrahydroxoaluminate ion to generate more hydroxide ions [25]. Based on this speculation, the reaction equation is described as follows.

$$Al^{3+} + 4OH^- \rightarrow \left[Al(OH)_4\right]^- \quad (1)$$

$$Ca_{10}(PO_4)_6(OH)_2 + \left[Al(OH)_4\right]^- \rightarrow Ca_{10}(PO_4)_6OH\cdot Al(OH)_4 + OH^- \quad (2)$$

During the defluoridation procedure, electrostatic adsorption can be encouraged as positively charged filtering material contacts with F^-. Also, the large number of -OH functional groups in the crystal lattices are capable of conducting replacement reaction or ion exchange reaction with F^- in water. In addition, $[Al(OH)_4]^-$ and $Ca_{10}(PO_4)_6OH\cdot Al(OH)_4$ is produced during the copolymerization process of this kind of material, which makes it possible for the occurrence of chemical adsorption between them and fluoride ions. Moreover, HAP-PAC copolymerization material is also accompanied by the generation of hydrolytic condensation product $[Al_{13}O_4(OH)_{24}]^{7+}$ and gel $[Al(OH)_3]$ [26]. The ligand hydroxyl ions embedded in these products can exchange with fluorine ions.

Based on the comprehensive analysis of these three kinds of filtering materials, it can be theorized that the

defluorination process of H1 is dominated by chemical adsorption and partly accompanied by physical adsorption, of which the main reaction equations are expressed as below (7-12); both electrostatic adsorption and partial chemical adsorption will occur during the defluorination process of H2, its reaction equations being shown as below (3-12); physical adsorption is the main reaction form on the surface of H3 when contacting with F^- (Plus, unbroken ingredients of HAP may also conduct relatively weaker electrostatic adsorption and ion exchange process), its chief reaction equations are conveyed as below (3-6).

Physical adsorption process:

$$\left[Al_xCa_{10-x}(PO_4)_6Cl_y(OH)_z\right]^{(x+2-y-z)+} + nF^- \rightarrow \left[Al_xCa_{10-x}(PO_4)_6Cl_y(OH)_z\right]^{(x+2-y-z)+} \cdots nF^- \quad (3)$$

$$\left[Al_xCa_{10-x}(PO_4)_6Cl_y(OH)_z\right]^{(x+2-y-z)+} + (x+2-y-z)F^- \rightarrow \left[Al_xCa_{10-x}(PO_4)_6Cl_y(OH)_z\right]\cdots F_{x+2-y-z} \quad (4)$$

$$Ca_{10}(PO_4)_6(OH)_2 + nF^- \rightarrow Ca_{10}(PO_4)_6(OH)_2 \cdots nF^- \quad (5)$$

$$\left[Al_2(OH)_nCl_{6-n}\right]_m + nF^- \rightarrow \left[Al_2(OH)_nCl_{6-n}\right]_m \cdots nF^- \quad (6)$$

Chemical adsorption process:

$$\left[Al_xCa_{10-x}(PO_4)_6Cl_y(OH)_z\right]^{(x+2-y-z)+} + mF^- \rightarrow \left[Al_xCa_{10-x}(PO_4)_6Cl_y(OH)_{z-m}F_m\right]^{(x+2-y-z)+} + mOH^- \quad (7)$$

$$[Al_xCa_{10-x}(PO_4)_6Cl_y(OH)_z]^{(x+2-y-z)+} + zF^- \rightarrow [Al_xCa_{10-x}(PO_4)_6Cl_yF_z]^{(x+2-y-z)+} + zOH^- \quad (8)$$

$$Ca_{10}(PO_4)_6OH\cdot Al(OH)_4 + xF^- \rightarrow Ca_{10}(PO_4)_6(OH)_{1-y}F_y\cdot Al(OH)_{4-x+y}F_{x-y} + xOH^- \ (0\le y\le 1, 0\le x\le 5) \quad (9)$$

$$\left[Al(OH)_4\right]^- + xF^- \rightarrow \left[Al(OH)_{4-x}F_x\right]^- + xOH^- \ (0\le x\le 4) \quad (10)$$

$$\left[Al_{13}O_4(OH)_{24}\right]^{7+} + xF^- \rightarrow Al_{13}O_4(OH)_{24-x}F_x^{7+} + xOH^- \ (0\le x\le 24) \quad (11)$$

$$Al(OH)_3 + xF^- \rightarrow Al(OH)_{3-x}F_x + xOH^- \ (0\le x\le 3) \quad (12)$$

HAP-PAC copolymerization material can trap the particles in water during the procedure of defluorination. Then these particles, treated as adsorbates, will precipitate together with the materials. Through this inner mechanism, the goal of fluoride removal in water can be thoroughly achieved. The general procedure of fluoride removal is illustrated in Fig. 10.

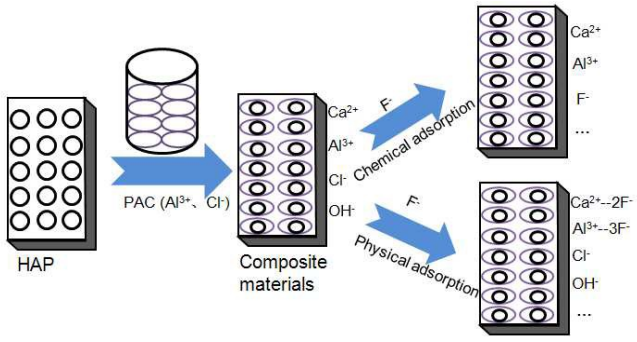

Fig. 10 Mechanism of fluoride removal by HAP-PAC copolymerization material

4 Conclusion

(1) A novel adsorbent of copolymerized HAP-PAC material is featured by strong defluorination capacity, thus enormously improving the defluoridation capacity of HAP. At the same time, by virtue of the strong flocculation effects of PAC, this material can eliminate the concern that powder materials may enter the water

supply network because of the difficulty in entrapment or sedimentation, hence attaining the goal of thoroughly removing fluoride in water. Moreover, the quality of the processed water can meet the standards of drinking water casting away any safety concern. It obviously provides a new method and an original idea for the preparation of high-efficiency fluoride removal material.

(2) The copolymerized HAP-PAC material prepared by means of aluminum chloride crystallization is characterized by the chemical combination between hydroxyapatite and poly aluminum chloride, and certain amount of Ca^{2+} and OH^- in HAP crystal lattice is partially doped and replaced by Al^{3+} and Cl^- in PAC. The structure of the copolymerization material possesses a highly homogeneous structure. Plus, its highest DC can reach up to 18.12 mg/g when the Al/Ca molar ratio is 0.22, an increase of 14.02 mg/g as compared with pure hydroxyapatite, and the fluoride removal process is mainly dominated by chemical adsorption process (ion exchange).

(3) As for the filtering material prepared by bauxite, a small part of Ca^{2+} and OH^- in HAP crystal lattice are doped and replaced by Al^{3+} and Cl^- in PAC, and both chemical combination and physical combination will occur during this procedure while the degree of uniformity is relatively weaker on account of the co-existence of HAP, PAC, and copolymerization material. The maximum DC is 13.72 mg/g at the optimal Al/Ca molar ratio 0.22. Electrostatic attraction and ion exchange are two main forms during the process of defluorination.

(4) In consideration of the filtering material prepared by physical mixing, the combination between HAP and PAC is mainly physical effects, with its highest DC reaching 13.08 mg/g at the best Al/Ca molar ratio 0.132. Physical adsorption is the governing form during the procedure of defluorination.

Acknowledgments

This work was supported by Jiangsu Province Science and Technology Key Research Program (Grant No. BE2015628), the 111 Project (B12030), the Fundamental Research Funds for the Central Universities (Grant No. 2014XT05), and the Priority Academic Program Development of Jiangsu Higher Education Institutions.

References

[1] Y. Ma, S. Wang, M. Fan, W. Gong and B. Gao, *J Hazard Mater*, 2009, **168**, 1140-1146.

[2] Y. Tang, X. Guan, T. Su, N. Gao and J. Wang, *Colloids and Surfaces A: Physicochemical and Engineering Aspects*, 2009, **337**, 33-38.

[3] W. Xiang, G. Zhang, Y. Zhang, D. Tang and J. Wang, *Chem Eng J*, 2014, **250**, 423-430.

[4] O. Barbier, L. Arreola-Mendoza and L. M. Del Razo, *Chem-Biol Interact*, 2010, **188**, 319-333.

[5] J. Zhu, H. Zhao and J. Ni, *Sep Purif Technol*, 2007, 56, 184-191.

[6] X. Zhao, L. Zhang, P. Xiong, W. Ma, N. Qian and W. Lu, *Micropor Mesopor Mat*, 2015, **201**, 91-98.

[7] S. Gao, J. Cui and Z. Wei, *J Fluorine Chem*, 2009, **130**, 1035-1041.

[8] S. Ghorai and K. K. Pant, *Sep Purif Technol*, 2005, **42**, 265-271.

[9] A. López Valdivieso, J. L. Reyes Bahena, S. Song and R. Herrera Urbina, *J Colloid Interf Sci*, 2006, **298**, 1-5.

[10] R. Leyva-Ramos, J. Rivera-Utrilla, N. A. Medellin-Castillo and M. Sanchez-Polo, *Chem Eng J*, 2010, **158**, 458-467.

[11] A. Bansiwal, D. Thakre, N. Labhshetwar, S. Meshram and S. Rayalu, *Colloids and Surfaces B: Biointerfaces*, 2009, **74**, 216-224.

[12] S. Meenakshi, C. S. Sundaram and R. Sukumar, *J Hazard Mater*, 2008, **153**, 164-172.

[13] M. Jiménez-Reyes and M. Solache-Ríos, *Water, Air, & Soil Pollution*, 2013, **224**, 1499-1454.

[14] D. Zhang, H. Luo, L. Zheng, K. Wang, H. Li, Y. Wang and H. Feng, *J Hazard Mater*, 2012, **241-242**, 418-426.

[15] J. Cheng, X. Meng, C. Jing and J. Hao, *J Hazard Mater*, 2014, **278**, 343-349.

[16] L. Chai, Y. Wang, N. Zhao, W. Yang and X. You, *Water Res*, 2013, **47**, 4040-4049.

[17] A. Bansiwal, P. Pillewan, R. B. Biniwale and S. S. Rayalu, *Micropor Mesopor Mat*, 2010, **129**, 54-61.
[18] W. Xu, L. Feng, M. Zhang and X. Wang, *Acta Sci Circumst*, 2013, **33**, 1570-1575.
[19] L. Feng, W. Xu, T. Liu and J. Liu, *J Hazard Mater*, 2012, **221-222**, 228-235.
[20] K. Pandi and N. Viswanathan, *Carbohyd Polym*, 2014, **112**, 662-667.
[21] Y. Nie, C. Hu and C. Kong, *J Hazard Mater*, 2012, **233-234**, 194-199.
[22] W. Xu, L. Feng and T. Liu, *Chin J Environ Eng*, 2012, **6**, 2351-2355.
[23] D. Huang, S. Quan, L. Liu, X. Li and W. Xie, *Inorg Chem Ind*, 2009, **41**, 18-21.
[24] H. Li, Y. Yang, S. Yang, A. Chen and D. Yang, *J Spectros*, 2014, **2014**, 1-7.
[25] Y. S. Ho, *Water Res*, 2006, **40**, 119-125.
[26] C. Zha, S. Zhang, M. Xia and L. Zhang, *Water Purif Technol*, 2005, **24**, 46-48.